communications physics

ARTICLE

https://doi.org/10.1038/s42005-022-00916-0 OPEN

Enhancement and manipulation of optical interaction between coupled nano-waveguides in hollow-core fibers

Shangran Xie [1,2]✉, Ran Gao[3] & Yi Jiang[1,2]

Optomechanical forces between evanescently coupled nano-waveguides serve as useful mechanisms to configure versatile functionalities of macro- and nano-devices. Strategies for boosting the optomechanical interaction strength are particularly compelling for the field of nanotechnologies. Here we show that the optical coupling strength between nano-waveguides can be enhanced by orders of magnitude when they are confined in hollow-core fibers. The presence of hollow core greatly increases the overlap integral between the nano-waveguides through excitation of the core modes. The excited higher-order core modes are able to mediate a long-range optomechanical interaction between the waveguides even though they are separated by tens of optical wavelength. It is found that the optical forces between the nanofibers can be switched from attractive to repulsive ones purely by tuning the gap between the nanofibers due to the optomechanical back-action effect induced by the higher-order core modes. The enhanced optomechanical coupling can be exploited to manipulate the collective eigenfrequencies of the coupled nano-waveguides via the optical spring effect. Our observation may find applications on the design of waveguide couplers embedded in the hollow core, or to realize miniaturized acoustic sensors.

[1] School of Optics and Photonics, Beijing Institute of Technology, 100081 Beijing, China. [2] Key Laboratory of Photonic Information Technology, Ministry of Industry and Information Technology, 100081 Beijing, China. [3] School of Information and Electronics, Beijing Institute of Technology, 100081 Beijing, China. ✉email: sxie@bit.edu.cn

Optical forces between coupled nano-waveguides have drawn intense interests for the field of optomechanics. Originated from the evanescent coupling between the waveguides, the generated optical gradient forces can be used to manipulate the mechanical motion of the waveguides, permitting demonstration of varieties of waveguide-based optical components, such as optical couplers[1], isolators[2], optical diodes[3], etc. The magnitude of the involved optical forces is intrinsically determined by the strength of mutual optical coupling. The sign of the optical forces can be adjusted via tuning the phase difference between the fields in waveguide[4]. It is highly beneficial to further boost the coupling strength and thus the optical forces since they are directly linked to the amplitude of the accessible mechanical motion[5].

Under this context, an effect of self-induced back-action trapping to enhance the optical forces on nano-objects have been reported[6,7]. It relies on the change of electric field as a feedback response to the object motion. The effect has been demonstrated in planar photonic crystal cavities[8] or nanoapertures in metallic film[6,9]. We have also proposed an optomechanical system in which tapered glass-fiber nanospikes or nanoplates are optically trapped in hollow-core fibers[10,11]. Arising from the optical interaction between the fiber nanospike or nanoplate and the hollow-core mode, a distinct type of optical trapping, namely optomechanical back-action trapping, has been demonstrated, showing a more than one order of magnitude increase in the strength of the optical forces. The enhancement of optical force results from the strong perturbation of the local electric field inside the hollow core as a result of the object motion and the back-action effects from the core modes. The interaction with a high-index nanoplate supporting internal optical open resonances in the hollow core opens up the possibility to form stably traps and anti-traps in the supermode field profile, behaving similarly to those experienced by cold atoms when the laser frequency is red or blue detuned of a nanoplate resonance. It has also been shown that plasmonic modes and hyperbolic metasurfaces can be exploited to enhance the optical trapping and binding forces[12–14]. Previous observations mainly focus on the effect of optomechanical back-action on individual single object. The effects of self-induced back-action on the collective dynamics between coupled objects have been largely unexplored.

Here we present a theoretical investigation on the optical coupling and optomechanical interactions between two nanofibers sitting in a hollow-core fiber, focusing on the collective phenomenon induced by the optomechanical back-action effect. It is found that the excited hollow-core mode can enhance the mutual optical coupling strength between the nanofibers and thus the optical forces acted on the nanofibers by more than two orders of magnitude. In sharp contrast with the previous observation that strong optical coupling can only occur when the two waveguides are in close vicinity with each other through evanescent waves, we show that excitation of the higher-order core modes can initiate an extended long-range optical interaction when the spacing between the nano-waveguides is orders of magnitude larger than the optical wavelength. The sign of the optical forces is demonstrated to be switched reversely when tuning the gap between the nano-waveguides in the hollow core.

Results and discussion

System configuration. The system is sketched in Fig. 1a. The hollow-core fiber is modeled as a silica capillary with inner diameter D. Each individual nanofiber (with diameter d) was considered as a uniform and lossless optical waveguide with length L. Global mechanical clamps (e.g., by fixing two ends of the nanofiber) with spring constant k_M are introduced to suspend the nanofibers forming clamped mechanical oscillators. The center-to-center gap between the nanofiber is set as g. The optical coupling between the nanofibers, mediated either by gradient forces induced by the evanescent fields, or by the optomechanical back-action effect in hollow core, is expected to introduce an additional optical spring k_O onto the fibers, further modifying their observed mechanical resonant frequencies. To demonstrate the enhanced coupling effect, we consider the case when the two nanofibers are symmetrically offset with respect to the core center along x direction, and laser light (with wavelength λ and power P) is launched into one of the nanofibers (Fig. 1b). Experimentally, such a system can be realized by inserting the nanofibers (some hundreds of nanometer in diameter) into the hollow core (tens of micrometer in diameter) from two ends of the hollow-core fiber following the scheme previously reported[10]. An alternate approach relies on the use of recently reported etching techniques to fabricate array of nanofibers or nanospikes on the endface of a multicore fiber[15]. Such a nanofiber array can be conveniently inserted into the hollow core using a translational stage with well-controlled precisions and optical accessibilities.

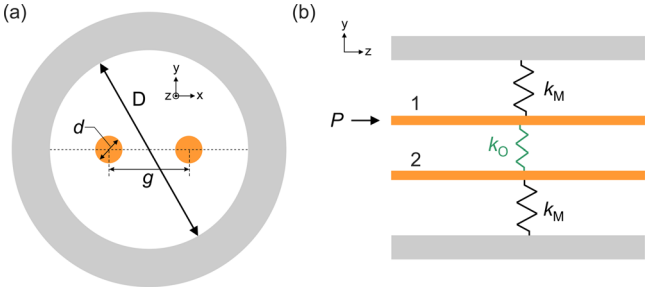

Fig. 1 Sketch of the considered optomechanical system. a Two nanofibers with diameter d (orange dots) are confined in a silica capillary with inner diameter D (gray). The center-to-center gap between the nanofibers is set as g. **b** The nanofibers are considered as being clamped by a mechanical spring with stiffness k_M. The optical coupling induces an additional optical spring k_O. Laser beam with wavelength λ and power P is coupled into nanofiber 1. All results still apply when light is coupled into nanofiber 2.

Coupling coefficient and energy transfer ratio. The optical coupling between the two nanofibers in the hollow core can be modeled by the scalar coupled mode equation:

$$\begin{aligned}\frac{da_1}{dz} &= i\beta_1 a_1 + i\kappa_{12} a_2 \\ \frac{da_2}{dz} &= i\kappa_{21} a_1 + i\beta_2 a_2\end{aligned} \tag{1}$$

where a_1 and a_2 is the electric field amplitude of the optical mode given by nanofiber 1 and 2, $\beta_1 = \beta_2 = \beta$ is the propagation constant of each individual "nanofiber plus hollow-core (NpHC)" supermode, $\kappa_{12} = \kappa_{21} = \kappa$ is the coupling constant between the nanofibers that can be calculated by the overlap integral between the NpHC modes[16]:

$$\kappa = \frac{1}{4}\sqrt{\frac{\varepsilon_0}{\mu_0}}\frac{k_0}{\sqrt{N_1 N_2}}\int_A (\varepsilon - \varepsilon_0)\boldsymbol{E}_1 \cdot \boldsymbol{E}_2 dA \tag{2}$$

where ε_0 and ε are the vacuum and relative permittivity, μ_0 is the vacuum permeability, k_0 is the vacuum wave vector, $\boldsymbol{E}_i$ is the electric field of the ith NpHC mode, N_i is the normalization parameter in terms of optical power[17]:

$$N_i = \frac{1}{2}\left|\int_A (\boldsymbol{E}_i \times \boldsymbol{H}_i) \cdot \hat{\boldsymbol{z}} dA\right| \tag{3}$$

$\boldsymbol{H}_i$ is the magnetic field of the ith NpHC mode, $\hat{\boldsymbol{z}}$ is the unit vector

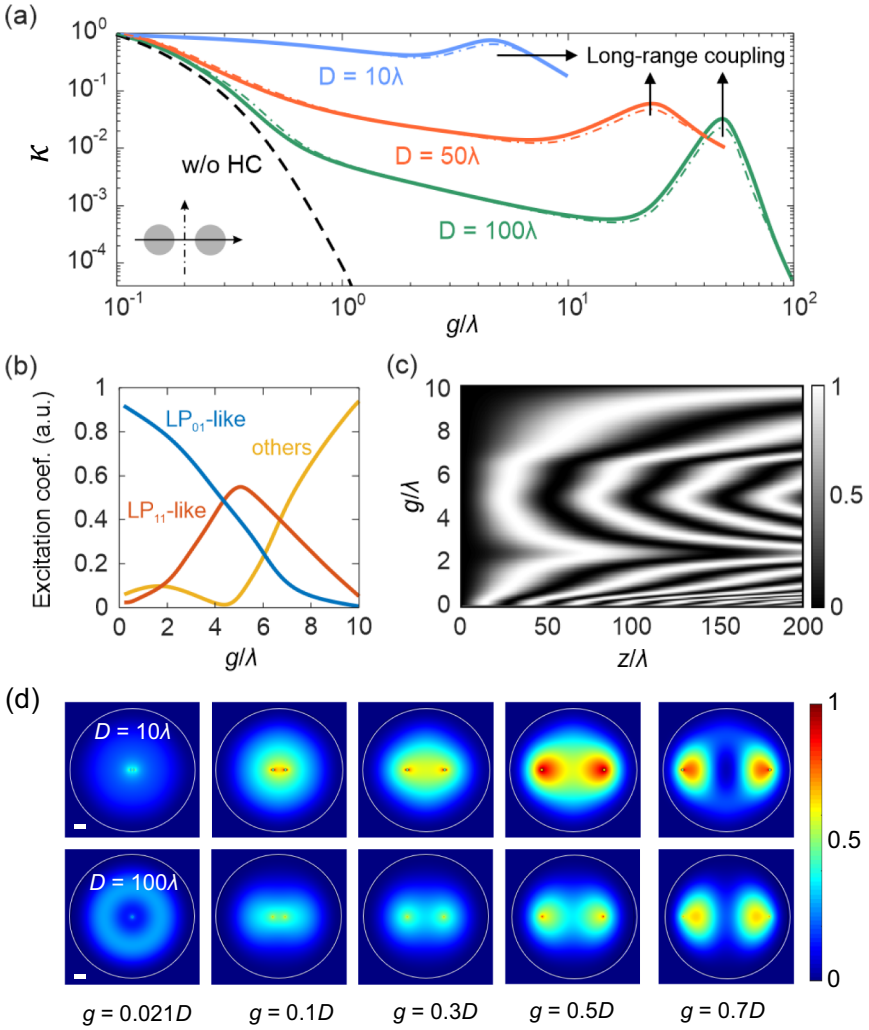

Fig. 2 The optical coupling coefficient and supermodes. a Normalized coupling constant κ versus the normalized gap g/λ between nanofibers for different core diameters. The diameter of the nanofiber is 0.2λ. The solid and dotted lines represent the case for electric field polarization along horizontal and vertical directions. The dashed line plots the case without hollow-core (HC) fiber. **b** Excitation coefficient of the LP_{01}-like, LP_{11}-like, and summation of all the rest core modes versus g/λ when $D = 10\lambda$. **c** Normalized power transfer ratio between the nanofibers versus propagation distance z and their gap g. **d** Simulated spatial distribution of the z-component of the Poynting vector for different values of g in the case of $D = 10\lambda$ (upper) and $D = 100\lambda$ (lower). The electric field polarizations for (**b**), (**c**), and (**d**) are in horizontal direction.

along z direction. The integration is performed over the entire area of the hollow core (A).

Figure 2a compares the calculated coupling constant κ versus normalized gap g/λ for different hollow-core diameters D. The diameter of the nanofiber was set as $d = 0.2\lambda$. The solid and dotted lines represent the case for the electric field polarization in the horizontal and vertical directions, respectively. It can be seen that κ can be enhanced by more than 100 times when D is decreased from 100λ to 10λ. To understand the mechanism of this enhancement, the upper and lower panel of Fig. 2d plot the simulated spatial distribution of the z-component of Poynting vector (S_z) inside the hollow core under different g values when $D = 10\lambda$ and 100λ, respectively. The electric field polarization is along horizontal direction. It can be seen that the launched laser light into one of the nanofibers can excite a combination of core modes. Figure 2b plots the calculated excitation efficiency (see "Methods") to the LP_{01}-like, LP_{11}-like and summation of all the rest core modes of the "two-nanofiber plus hollow-core (2NpHC)" structure, as a function of g/λ. When the nanofibers are placed close to the core center, the launched light mostly excites the fundamental core mode. The overlap integral between the nanofibers (which determines their optical coupling) in the hollow core, as it can be seen in Fig. 2d, not only depends on the evanescent field of each individual nanofiber but also on the excited mode profile. Since the core modes fill the entire space inside the hollow core, the overlap integral still exists even though the direct evanescent interaction between the nanofibers vanishes. This effect is clearly demonstrated in Fig. 2a by comparing the cases with and without hollow core. The dashed line in Fig. 2a plots the situation without hollow core, showing a typical exponential decay of κ with the increasing gap. In the case of $D = 10\lambda$, surprisingly, κ is found only slightly decreased when g/λ is increased from 0.2 to 1.

Furthermore, since the optical modes are strictly confined in the hollow core, the change in the excitation condition induced by the nanofibers is expected to strongly perturb the optical field in the core. A better confinement of the core mode (thus with a smaller core diameter D) can offer stronger back-action effects to enhance the optical coupling. This can be seen in Fig. 2d that the mode intensity in the case of $D = 10\lambda$ is several times stronger than the case of $D = 100\lambda$, indicating a larger value of overlap integral for smaller core diameter.

When the gap between the nanofibers is increased, regardless of the core diameter, the nanofiber starts to excite the LP_{11}-like core mode. This is evident in Fig. 2d showing that in both cases of $D = 10\lambda$ and 100λ, with the increasing of g, the intensity distribution gradually transits to a double-lobe profile. Note that in the case of $D = 100\lambda$, even though the nanofiber locates close to the core center, the LP_{02}-like mode rather than LP_{01}-like supermode is excited due to its larger overlap with the nanofiber mode. The excitation of the higher-order core mode opens up a new channel for the long-range optical coupling between the nanofibers. The two lobes of the LP_{11}-like core mode enables an indirect energy transfer between the nanofibers even though $g/\lambda \gg 1$. Figure 2c displays the normalized power transfer ratio between the two nanofibers over propagation distance along z direction for different gap values. The electric field polarization was set along the horizontal direction. A periodic behavior of the power transfer between the nanofibers can be clearly observed. With the increasing g value, κ first decreases due to the loss of evanescent coupling, while when reaching the long-range coupling regime, visible power transfer can be recovered appearing as a reduced coupling period. This highlights the possibility of exploiting the system as an efficient directional coupler even when the gap between the nanofiber is orders of magnitude larger than the laser wavelength. Note that the optimal values of g/λ achieving the maximum κ in the long-range coupling regime is given by the position of the two lobes of the LP_{11}-like core mode and is therefore connected with the core diameter.

Optomechanical forces. The net optical force acted on each nanofiber (in unit of N/m) can be calculated by integrating the Maxwell stress tensor $\mathbf{T}$ along its surface S:

$$f_O = \oint_S \langle \mathbf{T}(\mathbf{r}) \rangle \cdot d\mathbf{S} \tag{4}$$

A normalized optical force can be expressed via a proper normalization by the optical power:

$$\hat{f}_O = \frac{f_O c}{n_{\text{eff}} P_{SM}} \tag{5}$$

where c is the vacuum speed of light, n_{eff} is the effective mode index of the coupled waveguides, P_{SM} is the optical power coupled into the 2NpHC supermode. $\hat{f}_O$ corresponds to the efficiency of momentum transfer to the nanofiber[18]. The circles in Fig. 3a plot the optical forces acted on the nanofiber versus normalized gap g/λ under different core diameters calculated using Eqs. (4) and (5). Without the hollow core (black circles), the optomechanical force vanishes rapidly due to the loss of the evanescent coupling, while within the hollow core the optical forces can be greatly enhanced due to the confinement of optical modes. For the case of short-range interaction, the enhancement is mediated by the optomechanical back-action effect since the motion of nanofiber strongly perturbs the local electric field in the core. Figure 3b plots the calculated effective mode index of the LP_{01}- (solid lines) and LP_{11}-like (dotted lines) supermode. It can be seen that the modulation strength of the refractive index for the 2NpHC supermode is much stronger comparing to without hollow core (dashed line). The optical forces can be further calculated using the response theory at the laser frequency ω[19]:

$$\hat{f}_O = \sum_j \frac{P_j}{c} \frac{dn_{\text{eff},j}}{dg}\bigg|_\omega \tag{6}$$

where the summation is taken over different orders of the excited hollow-core modes. In the calculation, the excitation coefficients of the LP_{01}- and LP_{11}-like supermode (Fig. 1b) have been used as the weighting parameters to take into account the fractional power launched into the two modes. The solid lines in Fig. 3a plot the calculated optical forces using Eq. (6), agreeing reasonably well with the results from Maxwell stress tensor. The discrepancy can be attributed by the contribution of other core modes which are neglected in the calculation. Interestingly, the optical forces can be switched from attractive to repulsive forces when tuning from short-range to long-range interaction. The shaded areas in Fig. 3a indicate the regime of repulsive optical forces between the nanofibers. This is caused by the π phase difference between the electric field in the two lobes of the excited LP_{11}-like mode. In this case, due to the absence of intensity gradient from the evanescent field, the repulsive force is purely induced by the out-of-phase double-lobe core modes and the subsequent optomechanical back-action.

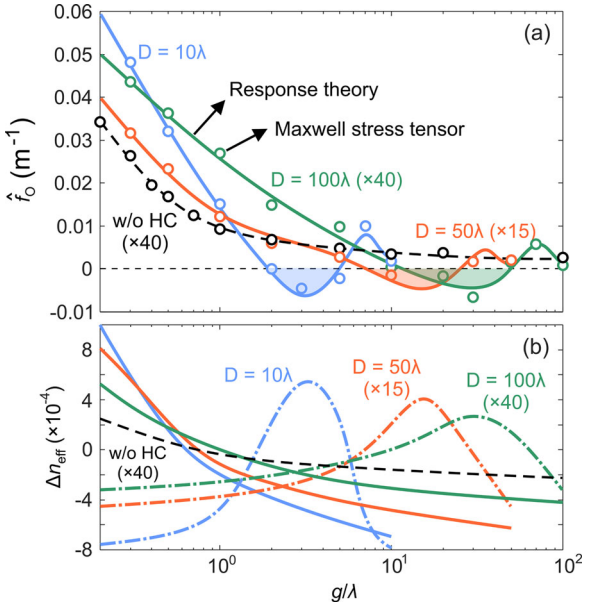

Fig. 3 The optomechanical forces and back-action. a Calculated optical forces using Maxwell stress tensor (circles) and response theory (solid lines) acted on the nanofibers versus their gap g/λ for different core diameters. The shaded areas indicate the regime that the nanofibers experience repulsive forces between each other. **b** Change in the effective refractive index of the LP_{01}-like (solid lines) and LP_{11}-like (dotted lines) core mode versus g/λ. The black-dashed lines in both (**a**) and (**b**) represent the case without hollow core (HC).

Optical spring effect. The optical forces between the nanofibers are expected to modify the equilibrium position of the nanofibers. Given the launched optical power, the equilibrium position is determined by the balance between the optical and mechanical restoring forces. Even though the inter-modal beating effect is expected to introduce a periodically modulated optical force and thus local flexural deflections along the nanofiber, it is a second-order effect comparing to the overall shift of nanofiber equilibrium position. An averaged optical force over many modulation periods along z direction is therefore considered for simplicity for the further analysis of the optical spring. At the equilibrium position, the optical spring was estimated by displacing each individual nanofiber in the vicinity of its equilibrium position along x direction and then calculating the corresponding changes in the optical forces acted on them. Following the scheme of coupled mechanical oscillators, the stiffness matrix of the nanofiber array can be written as:

$$[\mathbf{k}] = \begin{bmatrix} k_M + k_O & -k_O \\ -k_O & k_M + k_O \end{bmatrix}. \tag{7}$$

The observed resonant frequency can be solved by calculating the eigenvalue of $[\mathbf{k}]$. Note that the nanofiber can also oscillate in

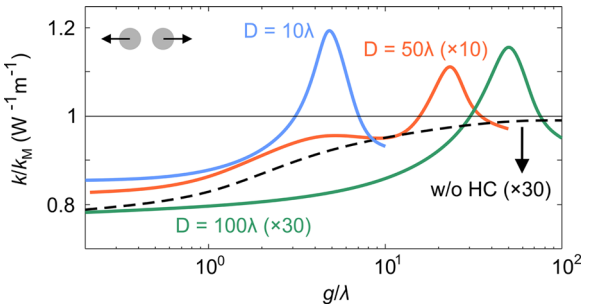

Fig. 4 The optical spring effect. Total nanofiber stiffness normalized by k_M versus gap g/λ for different core diameters for the out-of-phase collective eigenmode. The black-dashed line represents the case without hollow core (HC).

the y–z plane, and the two-dimensional motions are not fully decoupled due to the excitation of the hollow-core modes. While the estimated cross-term optical spring, thus $-\partial f_O/\partial y$ is more than 20 times smaller than the value of k_O in Eq. (7) for the scanned range of g/λ even for the case of $D = 10\lambda$, indicating a rather weak mutual coupling between x and y motions. The mechanical dissipation term has also been neglected in the analysis. The eigenvalue for the in-phase collective motion of the two nanofiber is simply k_M since the optical spring does not take effect. For the out-of-phase motion, Fig. 4 plots the normalized mechanical stiffness to k_M (in unit of W^{-1} m^{-1}) versus the gap and the hollow-core diameter. It can be seen optomechanical interaction can both increase or decrease the nanofiber stiffness depending on the relative gap value. In short-range interactions, the attractive optical force introduces anti-trapping effect on the nanofiber, decreasing the overall mechanical stiffness. While in the long-range coupling regime, the repulsive optical forces are found to increase the mechanical stiffness. It is evident that the optical spring effect is orders of magnitude stronger within the hollow core due to the back-action effect comparing to the case without hollow core (black-dashed line).

Conclusions. Order-of-magnitude enhancement of the optical coupling strength and collective effects of coupled nano-waveguides confined in hollow-core fiber are reported. The results show that the effect of optomechanical back-action opens up new degrees of freedom to manipulate both the strength and direction of optical forces acted on nano-objects in the hollow core. The enhanced long-range optical coupling can be used to design directional couplers with the gap between nano-waveguides orders of magnitude larger than the laser wavelength, bringing in great convenience and reconfigurability to waveguide-based coupling devices. The coupler may be achieved by inserting the nanofibers (with standard single-mode fiber pigtails) from two ends of hollow-core fiber and routing light from one to another with a continuously tunable coupling efficiency. The ability of tuning the sign of the optical forces via excitation of the hollow-core modes can be exploited to tailor the mechanical properties (such as resonant frequency, quality factor, etc.) of the nanofiber. Under this context, through inserting the fabricated nanospike array into the hollow core[15], the resonant frequency of each individual nanospike can be vastly tuned by the enhanced optomechanical interaction, leading to a multi-frequency, reconfigurable and miniaturized acoustic sensor. The optomechanically active nanofibers can also be applied to couple higher-order core modes into hollow-core fiber in a controlled manner. Finally, the presented results on two nano-waveguides can be feasibly extended to more waveguides or to chip-based platforms using a similar analysis procedure.

Methods

Calculation of the excitation efficiency to the hollow core modes. The excitation efficiencies to the hollow core modes by the nanofibers were calculated by overlapping the electric field distribution in the hollow core (E_{HC}) with that of the eigenmodes of the 2NpHC structure:

$$\eta_i = \frac{\left|\int_A E_{HC} E^*_{SM,i} dA\right|^2}{\int_A |E_{HC}|^2 dA \int_A |E_{SM,i}|^2 dA} \quad (8)$$

where $E_{SM,i}$ is the electric field distribution of the ith 2NpHC eigenmode. Both E_{HC} and $E_{SM,i}$ were obtained by finite element modeling of the geometric structure shown in Fig. 1a.

Data availability

Data underlying the results presented in this paper are not publicly available at this time but may be obtained from the authors upon reasonable request.

Code availability

The computer codes to simulate the coupling coefficients, optomechanical forces and optical spring effects are available from the corresponding authors upon reasonable request.

Received: 25 October 2021; Accepted: 16 May 2022;
Published online: 30 May 2022

References

1. Fong, K. Y., Pernice, W. H., Li, M. & Tang, H. X. Tunable optical coupler controlled by optical gradient forces. *Opt. Express* **19**, 15098–15108 (2011).
2. Ruesink, F., Miri, M. A., Alu, A. & Verhagen, E. Nonreciprocity and magnetic-free isolation based on optomechanical interactions. *Nat. Comm.* **7**, 1–8 (2016).
3. Qiu, H., Dong, J., Liu, L. & Zhang, X. Energy-efficient on-chip optical diode based on the optomechanical effect. *Opt. Express* **25**, 8975–8985 (2017).
4. Li, M., Pernice, W. H. P. & Tang, H. X. Tunable bipolar optical interactions between guided lightwaves. *Nat. Photon.* **3**, 464–468 (2009).
5. Butsch, A., Conti, C., Biancalana, F. & St. J Russell, P. Optomechanical self-channeling of light in a suspended planar dual-nanoweb waveguide. *Phys. Rev. Lett.* **108**, 093903 (2012).
6. Juan, M. L., Gordon, R., Pang, Y., Eftekhari, F. & Quidant, R. Self-induced back-action optical trapping of dielectric nanoparticles. *Nat. Phys.* **5**, 915–919 (2009).
7. Neumeier, L., Quidant, R. & Chang, D. E. Self-induced back-action optical trapping in nanophotonic systems. *N. J. Phys.* **17**, 123008 (2015).
8. Descharmes, N., Dharanipathy, U. P., Diao, Z., Tonin, M. & Houdré, R. Observation of backaction and self-induced trapping in a planar hollow photonic crystal cavity. *Phys. Rev. Lett.* **110**, 123601 (2013).
9. Chen, C. et al. Enhanced optical trapping and arrangement of nano-objects in a plasmonic nanocavity. *Nano Lett.* **12**, 125–132 (2012).
10. Xie, S., Pennetta, R. & St. J. Russell, P. Self-alignment of glass fiber nanospike by optomechanical back-action in hollow-core photonic crystal fiber. *Optica* **3**, 277–282 (2016).
11. Günendi, M. C., Xie, S., Novoa, D. & St. J. Russell, P. Optical traps and anti-traps for glass nanoplates in hollow waveguides. *Opt. Express* **27**, 17708–17717 (2019).
12. Kostina, N. A. et al. Nano-scale tunable optical binding mediated by hyperbolic metamaterials. *ACS Photon.* **7**, 425–433 (2020).
13. Jiang, M. et al. Two-dimensional arbitrary nano-manipulation on a plasmonic metasurface. *Opt. Lett.* **43**, 1602–1605 (2018).
14. Kostina, N. et al. Optical binding via surface plasmon polariton interference. *Phys. Rev. B* **99**, 125416 (2019).
15. Wang, Z. et al. Optically addressable array of optomechanically compliant glass nanospikes on the endface of a soft-glass photonic crystal fiber. *ACS Photon* **6**, 2942–2948 (2019).
16. Okamoto, K. *Fundamentals of Optical Waveguides* (Academic, 2006).
17. Snyder, A. W. & Love, J. D. *Optical Waveguide Theory* (Chapman and Hall, 1983).
18. Ashkin, A. Forces of a single-beam gradient laser trap on a dielectric sphere in the ray optics regime. *Biophys. J.* **61**, 569–582 (1992).
19. Rodrigues, J. R. & Almeida, V. R. Optical forces through the effective refractive index. *Opt. Lett.* **42**, 4371–4374 (2017).

Acknowledgements
This work is funded by the Science and Technology Innovation Program of Beijing University of Technology (No. 3040012212113).

Author contributions
S.X. conceived the idea, developed the theoretical models, and made the calculations. S.X., R.G., and Y.J. participated in the scientific discussion and together wrote the manuscript.

Competing interests
The authors declare no competing interests.

Additional information
Correspondence and requests for materials should be addressed to Shangran Xie.

Peer review information *Communications Physics* thanks David Grass and the other, anonymous, reviewer(s) for their contribution to the peer review of this work.

Reprints and permission information is available at http://www.nature.com/reprints

Publisher's note Springer Nature remains neutral with regard to jurisdictional claims in published maps and institutional affiliations.